

# SEPARATION AND SLIDING BETWEEN SOIL AND STRUCTURE TO STRONG EARTHQUAKE MOTION

Kenzo Toki<sup>I</sup>, Tadanobu Sato<sup>II</sup> and Fusanori Miura<sup>III</sup>

## SUMMARY

This paper presents a general method for the seismic response analysis of soil-structure systems considering separation and sliding phenomena at the interface between soil and structure by using the finite element method. Joint elements which have properties such that tensile forces are not transmitted between two planes are adopted to express these phenomena. The seismic response of two soil-structure models are dealt with to illustrate the applicability of the method to the actual soil-structure system and the effect of sliding and separation phenomena on the dynamic stability of the systems are examined.

## 1. INTRODUCTION

Most studies concerned with soil-structure interaction assume a perfect bond on the contact surface between soil and structure. But in the actual system, the separation and sliding phenomena may occur during strong earthquake motion, and then the response of the soil-structure system associated with sliding and separation will be greatly different from the response with a perfect bond assumption at the interface. From the above point of view, several analytical research works have been performed for the separation and sliding phenomena in the dynamic problem. However, these works are not always applicable to all kinds of actual soil-structure systems<sup>1-3</sup>.

The purpose of this study is to present an effective analysis procedure for the soil-structure system including the possibility of separation and sliding at the interface between soil and structure by use of the joint element. The method is applied to a model of a reactor building resting on the ground surface and to a buried foundation structure, and the stability of such structure with respect to sliding and overturning is discussed in detail.

## 2. APPLICATION OF THE JOINT ELEMENT

Fig. 1 shows a joint element constructed from four nodal points I, J, K and L<sup>4</sup>). Two pairs of nodal points I-L and J-K are assumed to occupy the same coordinate at the initial state, that is, two surfaces I-J and K-L are in contact. The behaviour of the contact surface between soil and structure is expressed by the relative position of both surfaces of the joint element. The relative motion of both surfaces is classified as follows:

- (i) parallel motion to the joint wall (sliding between soil and structure)
- (ii) perpendicular motion to the joint wall (separation and contact)
- (iii) rotational motion around the center of the joint element.

The deformation characteristics of the joint are determined by the stiffness

---

I Professor, Disaster Prevention Res. Inst., Kyoto Univ., Uji, Kyoto, Japan  
II Associate Professor, ditto.      III Research Associate, ditto.

of the shear direction  $K_S$ , the normal direction  $K_N$  and the rotational component  $K_\omega$ . Since  $K_\omega$  is expressed in terms of  $K_N$  the constitutive relation of the joint is expressed by two parameters  $K_S$  and  $K_N$ .

The stiffness matrix of joint element  $[K]_{s,n}$  is given by Eq. 1.

$$[K]_{s,n} = \frac{1}{4} \begin{pmatrix} K_S & 0 & K_S & 0 & -K_S & 0 & -K_S & 0 \\ & 2K_N & 0 & 0 & 0 & 0 & 0 & -2K_N \\ & & K_S & 0 & -K_S & 0 & -K_S & 0 \\ & & & 2K_N & 0 & -2K_N & 0 & 0 \\ & & & & K_S & 0 & K_S & 0 \\ \text{Symmetric} & & & & & 2K_N & 0 & 0 \\ & & & & & & K_S & 0 \\ & & & & & & & 2K_N \end{pmatrix} \quad (1)$$

The stiffness matrix  $[K]_{s,n}$  is determined in the local coordinates  $(s,n)$ , and should be transformed to the global coordinate system in actual use.

In performing the dynamic response analysis, the stress-strain characteristics of the joint are assumed as shown in Figs. 2(a) and (b) for the normal and shear component, respectively. The normal stress is not transmitted for  $\epsilon_o \geq 0$  (separation) and a linear constitutive relation based on the stiffness  $K_N$  is valid for  $\epsilon_o < 0$ . The spring coefficient  $K_N$  is related to the fictitious relative displacement of the structure past the interface into the soil region, which in actual response would not occur. Therefore  $K_N$  should be as large as possible<sup>5</sup>. Sliding will take place when the absolute value of shear stress reaches the yield stress  $\tau_y$ , and the linear shear stress-strain relation remains below this stress level. When separation occurs, the shear stress is not transmitted through the joint wall. The yield stress  $\tau_y$  is determined as a function of the normal stress assuming the Mohr-Coulomb criterion.

$$\begin{aligned} \tau_y &= C - \sigma_n \cdot \tan \phi, \text{ for } \sigma_n \leq 0 \text{ (compression)} \\ \tau_y &= 0, \text{ for } \sigma_n > 0 \text{ (extension)} \end{aligned} \quad (2)$$

where  $C$  is the cohesion,  $\sigma_n$  is the normal stress and  $\phi$  is the angle of internal friction.

Considering the general dynamic response analysis of a linear system, it is sufficient to treat only the deformation from the static equilibrium condition. However, the initial stress has an important role in controlling the separation and sliding in the response analysis using the joint element. The initial stress induced by gravity forces should be taken into consideration and is calculated by using Boussinesq's equation in this study.

The numerical calculation, including the separation and sliding phenomena, shows strong non-linearity, and thus the equation of motion must be solved by the step by step integration method in time domain. The required time interval of each step is on the order of 0.001 seconds. Therefore, an excessive amount of computation time is necessary to calculate the seismic response. The load transfer method of iterative computation is found to be most effective in this analysis, in which the stiffness matrix is kept constant during the computation and only the external force is modified so as to satisfy the equilibrium condition. The computation of the inverse stiffness matrix is only once required at the first step of the response analysis and therefore the computation time is greatly reduced.

### 3. SEISMIC RESPONSE ANALYSIS

Fig. 3 shows a model 1, which is a structure resting on the ground surface. The model is a typical reactor building of a nuclear power station in Japan. Three joint elements are arranged along the interface between the structure and ground. A pier foundation of a long span bridge is model 2, shown in Fig. 4, in which eight joint elements are arranged along the interface. The model parameters are listed in Table 1 and 2 corresponding to models 1 and 2, respectively. The value of the governing quantities are listed in the bottom of Tables. Non-linear behaviour is only considered in joint elements and the structure and soil are assumed to behave as linear elastic materials. These two modeled structures are subjected to simultaneous excitation of NS and UD components of the El Centro (1940) accelerograms as well as sinusoidal excitations. The stability of structure for sliding and separation have been investigated and compared with the results estimated by a provisions for aseismic design of foundation structures.

#### 3.1 The response to sinusoidal excitation

(a) Response analysis of model 1 : Fig. 5 shows the amount of sliding at the contact surface and displacement at the center of gravity for the case  $\phi = 0^\circ$  and the horizontal sinusoidal excitation of 200 gal. The displacement at the C. G. of the linear system without joint elements is denoted by the smooth curve. The symbols  $\bullet$  and  $\circ$  correspond to the sliding and the displacement at the C. G., respectively. Both sliding and displacement decrease with increasing frequency and the difference between them is kept almost constant for variation of frequency. This result implies that the sliding will occur when the structure is inclined at a specified angle, whereas the rocking motion is predominant for the linear system. The sliding phenomenon disappears beyond a specified frequency for the given excitation level.

Lifting off and stability of overturning are also examined. Lifting off begins when the stress at the structure base vanishes. It doesn't appear, however, even for an input excitation of 400 gal for which the normal stress is still compressive. In addition, the same investigation carried out for the excitation level of 300 gal and a frequency of 3 Hz results into no occurrence of lifting off or sliding phenomenon.

(b) Response analysis of model 2 : Fig. 6 compares the displacement at structure top (point A in Fig. 4) for the case of  $\phi = 30^\circ$  and the excitation level of 300 gal. The response of the non-linear system is greater than that of the linear system for the frequency range below 6 Hz because sliding between the side wall of the structure and the soil takes place. The separation between the side wall and the soil near the ground surface occurs at 2 Hz, and then the displacement becomes greater than that of the linear system by 30 %. In the linear system, the motion of the structure is so strongly restrained by the surrounding soil that the response becomes smaller than that of the non-linear system containing joint elements, especially in the low frequency range.

#### 3.2 The response to seismic excitation

(a) Seismic response analysis of model 1 : Fig. 7 shows the horizontal displacement at point A (Fig. 3, where both side of structure and soil sharing the same point before shaking,  $\phi = 0^\circ$ ), The solid line indicates the displacement of the structure, and the broken line that of the soil. The relative

displacement between soil and structure becomes large from 1.7 to 2.5 sec, and after this period the structure vibrates with a constant residual deformation. In the figure, the displacement of the linear system is also shown by a long-short line. While the displacement of the structure becomes large when sliding occurs, the displacement of the soil is almost the same as that of the linear system. Fig. 8 illustrates the hysteresis loop for shear direction at point B ( $\phi = 0^\circ$ ). The point marked by S denotes the starting time and E the ending time of the response analysis. The residual value of relative displacement is 11 mm.

Although the calculated results for the case  $\phi = 30^\circ$  and  $C = 10 \text{ ton/m}^2$  are not shown in any figures or tables, sliding and lifting off did not occur in the response analysis. The minimum normal stress of  $38.6 \text{ ton/m}^2$  at the structure base (point B) is generated at a time 2.2 sec, and the shear stress is  $19.0 \text{ ton/m}^2$ . Therefore, if the internal friction angle is less than  $13.7^\circ$ , local sliding may take place merely in the vicinity of point B.

(b) Seismic response analysis of model 2 : The hysteresis loop at point C of model 2 is shown in Fig. 9 for case of  $\phi = 30^\circ$ . Fig 9(a) is for the shear direction and Fig. 9(b) for the normal direction. The separation at this point takes place from 1.88 to 2.02 sec. The shear stress vanishes suddenly at 1.88 sec and the sliding is remarkable to 2.02 sec. The slope of the hysteresis curve for the shear direction varies from time to time within the period of 2.14-2.24 sec, because the fluctuation of normal stress with time results in the change of yield stress of the contact surface. Separation and sliding between the base of the structure and the soil did not occur for the cases of  $\phi = 0^\circ$  or  $\phi = 30^\circ$ .

The horizontal displacement at the top of the structure of model 2 (point A in Fig. 4) is shown in Fig. 10. The solid line is for the linear cases, the long-short line for the case of  $\phi = 0^\circ$  and the broken line for the case of  $\phi = 30^\circ$ . The displacement for the cases of non-linear are greater than that of the linear case by 15-30 % at every peak, and the same results are obtained for the acceleration. This means that the analysis assuming perfect bond at the interface between structure and soil underestimates the quantity of structural response due to the overrestriction of structural movement by the sub-soil. This phenomenon is especially notable in long period excitation. Consequently, in order to preclude the possibility of the separation and sliding of soil-structure systems in practical design, special consideration should be paid to the seismic wave containing long period components.

### 3.3 Safety factor for sliding

Fig. 11 shows the safety factor for sliding of entire the structure (this factor will be referred to as total safety factor) of model 1 for the case of  $\phi = 30^\circ$  and the sinusoidal excitation amplitude of 245 gal, corresponding to a seismic coefficient of 0.25. The safety factor for sliding is computed as the ratio of the yield shear stress  $\tau_y$  to the shear stress  $\tau$ . The local safety factor is defined for each joint by the minimum value of this ratio through the analyzed time. The total safety factor is also defined by the maximum value among the local safety factor. Fig. 11 indicates that the total safety factor does not depend on the frequency. The broken line in the figure is obtained using the following equation obtained from typical technical guide lines for aseismic design of foundation structures<sup>6)</sup>.

$$S_F = \frac{\mu \cdot V}{H} \quad (3)$$

where  $\mu$  is the coefficient of friction,  $V$  is the vertical force and  $H$  is the horizontal force. Taking  $V$  as the weight of structure and  $H=k_h \cdot V$ ,  $S_F$  becomes 2.32 for  $\mu=\tan 30^\circ$  and  $k_h=0.25$ . This value of  $S_F$  is close to the total safety factor, and thus it may be concluded that the possibility of sliding of massive structures resting on the ground surface, such as model 1, can be ascertained by the seismic coefficient method.

Fig. 12 illustrates the safety factor of sliding between structural base and soil of model 2. The excitation is a sinusoidal wave with an amplitude of 245 gal. Since the total safety factor is greater than 10.0, the sliding of the entire structure does not occur, whereas the possibility of local sliding is rather higher. This is due to the decrease of normal stress at the contact surface, due to the rocking motion of the structure. The broken line is the statical safety factor based on the guide lines for the aseismic design of a caisson foundation with 70 m width. The value is greater than the total safety factor. One reason for this is the present guide line deals with the three dimensional structure, considering the shear restriction of the side wall in the direction of motion. In the finite element analysis, only two dimensional structure is treated and the side resistance parallel to the direction of motion is not taken into account. Therefore, the large relative displacement is generated along the contact surface and it may yield higher shear stresses.

The safety factor defined between the structural base and the soil, which was determined from the seismic response analysis, is illustrated in Fig. 13. The excitation is the El Centro accelerograms (1940, NS and UD comp.) scaled to 0.5, 2 and 3 times the original amplitude. The total safety factor is greater than 1.0 even for 3x excitation, while on the contrary the local safety factor becomes smaller than 1.0, thus indicating that sliding takes place. The local sliding is caused by the lifting off the structural base in the vicinity of the edge, due to the rocking motion. The overturning of the structure hardly occurs for the embedded structure such as model 2 in spite of the existence of local lifting off between structure base and ground.

#### 4. CONCLUSION

A general method for the seismic response analysis of soil-structure systems considering separation and sliding phenomena at the interface between soil and structure is developed in this study. From the analysis presented, the following can be concluded:

- (1) Dynamic separation and sliding at the interface between soil and structure becomes susceptible to analysis by use of the joint element in the finite element method.
- (2) In the analysis assuming perfect bond on the contact surface between soil and structure, the structure's motion is restricted by the surrounding sub-soil, thus possibly underestimating the actual response of the structure.
- (3) There is a specified frequency above which separation and sliding

does not take place, which depends on the excitation level. Separation and sliding becomes larger as the frequency becomes smaller than this specified frequency. Therefore, careful consideration should be paid, in the discussion of sliding and separation, to seismic excitations containing long period components.

(4) Safety for sliding may be examined by either the proposed analytical method or the guide lines for aseismic design of foundation structures. Both estimates of safety factor for sliding of the entire structure shows a good agreement. On the other hand, the safety for local sliding can not be checked by the method provided in the guide line. Therefore, application of the proposed method permits analysis of the progress of sliding of the structural system.

(5) The lifting off or the overturning of the structure is also examined, and a high safety factor is obtained for the two examples. Although not discussed in detail, it could be noted that these phenomena will be important parameters in the aseismic design of other types of structures such as tall buildings and towers.

Although the analytical examples presented herein have shown realistic behaviour for soil-structure systems including separation and sliding phenomena at the interface between soil and structure, there are many problems in performing the more rigorous response analysis. For instance, research on the yielding criteria and constitutive relation of the joint, on the effect of non-linearity of soil behaviour and on the extension to three dimensional analysis is necessary.

#### ACKNOWLEDGEMENT

The authors wish to express their sincere thanks to Prof. Yuzo Ohnishi of Kyoto University and Mr. Hideaki Kishimoto of Japan Computer Consultants, Osaka, for their suggestions regarding programming of the dynamic joint element.

#### REFERENCES

- 1) J.P. Wolf, 1976, 'Soil-structure interaction with separation of base from soil (lifting off)', Nuclear Engineering and Design 38, Holland Publishing Company, pp.357-384.
- 2) Y. Tsuboi, Y. Hangai, M. Takeda and M. Honma, 1978, 'A simple analytical method of walled structure considering up-lift of foundation', Proc. 5th Japan Earthquake Engineering Symposium, pp.1265-1272.
- 3) Y. Sasaki, Y. Fujino and M. Hakuno, 1978, 'Sliding of mass by seismic excitation -the influence of UD component-', Proc. Annual Meeting of the Japan Society of Civil Engineers (33rd) I-185, (in Japanese).
- 4) R.E. Goodmann, 1976, 'Method of geological engineering in discontinuous rocks', West Publishing Company, Ch.8, pp.300-368.
- 5) L.R. Herrmann, 1978, 'Finite element analysis of contact problems', Proc. ASCE, Vol.105, EM5, pp.1043-1057.
- 6) Report on the investigation of the aseismic design of the Honshu-Shikoku junction bridge, Sub-committee on the aseismic design of the Honshu-Shikoku junction bridge, The Japan Society of Civil Engineers, 1974, (in Japanese).

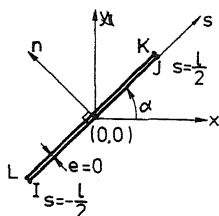


Fig.1 Configuration of joint element

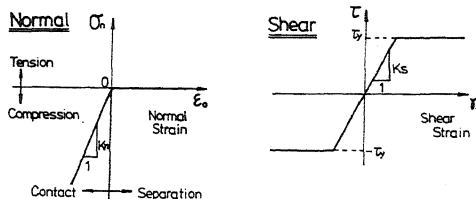


Fig.2 Relationship between stress and strain at midpoint of joint element

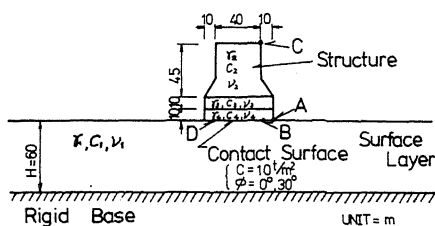


Fig.3 General view of soil-structure system Model 1

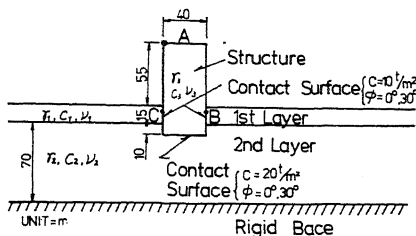


Fig.4 General view of soil-structure system Model 2

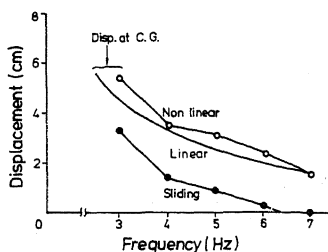


Fig.5 Frequency dependence of displacement at C. G. and sliding at the interface to horizontal sinusoidal excitation. ( $\phi=30^\circ$ , Excitation amplitude: 200 gal)

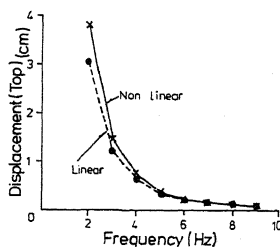


Fig.6 Displacement of structure at point A of Model 2 due to horizontal sinusoidal excitation. ( $\phi=30^\circ$ , Excitation amplitude: 300 gal)

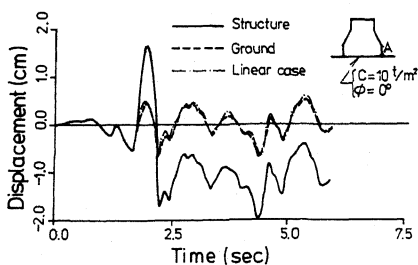


Fig.7 Horizontal displacement at point A of Model 1 due to El Centro accelerograms.

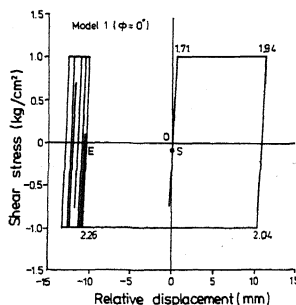
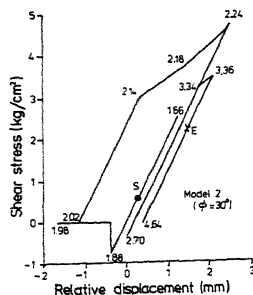
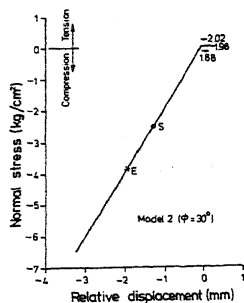


Fig.8 Hysteresis loop for shear direction at point B of Model 1.



(a) For shear direction



(b) For normal direction

Fig. 9 Hysteresis loop at point C of Model 2. ( $\phi=30^\circ$ )

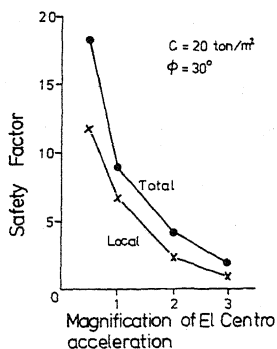


Fig. 13 Safety factor for sliding of Model 2 excited by El Centro accelerograms.

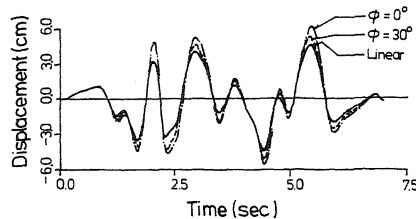


Fig. 10 Horizontal displacement at the top of structure. (Point A of Model 2)

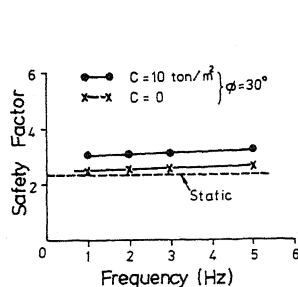


Fig. 11 Safety factor for sliding of Model 1. (Excitation amplitude: 245 gal)

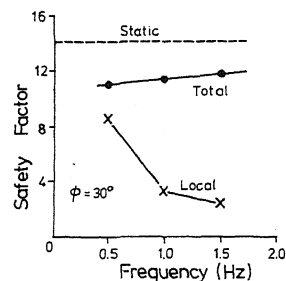


Fig. 12 Safety factor for sliding of Model 2. ( $\phi=30^\circ$ , Excitation amplitude: 245 gal)

Table 1 Physical properties of Model 1.

	Unit weight ( $\text{ton/m}^3$ )	Shear wave velocity (m/sec)	Poisson's ratio	Damping factor
Ground	$\gamma_1 = 1.8$	$C_1 = 500$	$\nu_1 = 0.4$	$h = 0.2$
Structure	$\gamma_2 = 0.75$ $\gamma_3 = 1.7$ $\gamma_4 = 2.4$	$C_2 = 1720$ $C_3 = 1600$ $C_4 = 1600$	$\nu_2 = 0.17$ $\nu_3 = 0.17$ $\nu_4 = 0.17$	$h = 0.05$
Joint	Shear spring coefficient $K_s = 518200 \text{ ton/m}^2$ Normal spring coefficient $K_n = 518200 \text{ ton/m}^2$ Cohesion $C = 10 \text{ ton/m}^2$ Internal friction angle $\phi = 0^\circ \text{ or } 30^\circ$			

Table 2 Physical properties of Model 2.

	Unit weight ( $\text{ton/m}^3$ )	Shear wave velocity (m/sec)	Poisson's ratio	Damping factor
Ground	$\gamma_1 = 1.8$ $\gamma_2 = 1.8$	$C_1 = 180$ $C_2 = 360$	$\nu_1 = 0.4$ $\nu_2 = 0.4$	$h = 0.2$
Structure	$\gamma_3 = 2.4$	$C_3 = 1600$	$\nu_3 = 0.17$	$h = 0.05$
Joint	Shear spring coefficient $K_s = 200000 \text{ ton/m}^2$ Normal spring coefficient $K_n = 200000 \text{ ton/m}^2$ Cohesion $C = 10 \text{ or } 20 \text{ ton/m}^2$ Internal friction angle $\phi = 0^\circ \text{ or } 30^\circ$			